

# Macroscopic Organohydrogel Hybrid from Rapid Adhesion between Dynamic Covalent Hydrogel and Organogel

Guohua Deng,<sup>\*,†</sup> Qian Ma,<sup>†</sup> Hongxia Yu,<sup>†</sup> Yunfei Zhang,<sup>†</sup> Zhichao Yan,<sup>‡</sup> Fuyong Liu,<sup>‡</sup> Chenyang Liu,<sup>\*,‡</sup> Huanfeng Jiang,<sup>†</sup> and Yongming Chen<sup>\*,§</sup>

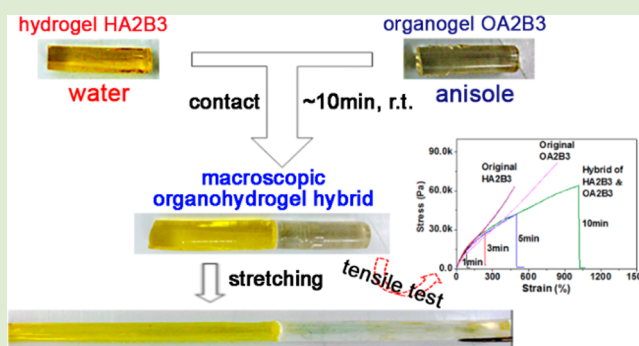
<sup>†</sup>School of Chemistry and Chemical Engineering, South China University of Technology, Guangzhou 510640, China

<sup>‡</sup>Beijing National Laboratory for Molecular Sciences, CAS Key Laboratory of Engineering Plastics, Joint Laboratory of Polymer Science and Materials, Institute of Chemistry, The Chinese Academy of Sciences, Beijing 100190, China

<sup>§</sup>Key Laboratory for Polymeric Composite and Functional Materials of Ministry of Education, School of Chemistry and Chemical Engineering, Sun Yat-Sen University, Guangzhou 510275, China

## S Supporting Information

**ABSTRACT:** A macroscopic organohydrogel hybrid was prepared by fast adhesion between the hydrogel and organogel which often repel each other. The two original gels were prepared by condensation of two poly(ethylene glycol) (PEG) gelators in anisole and water, respectively. Reversible acylhydrazone bonds formed in the condensation act as linking points of the polymer networks in the gels. When the two gels were brought into contact, a robust hybridized gel was obtained in 10 min. An emulsion layer formed at the interface between the two gels and dynamic chemistry of acylhydrazone bonding are key factors in rapid adhesion of the two inherently different gels. We hope this finding will enable the development of intelligent soft objects whose macroscopic water and oil phases contain different functional components.



Hydrogel and organogel are generally prepared by physical or chemical cross-linking of gelators in water or oil. Three-dimensional cross-linked networks thus formed provide skeletons for holding a large amount of solvents. Although hydrogels and organogels have attracted much interest in recent decades for their applications<sup>1</sup> in pharmaceuticals,<sup>2</sup> biotechnology,<sup>3–6</sup> and intelligent materials,<sup>7</sup> their macroscopic hybridization has never been found. This is because their main constituents, water and oil, are intrinsically immiscible. As reported in the literature,<sup>8–10</sup> macroscopic hybrid gels have been prepared by adhering or “gluing” different gels through noncovalent interactions, and thereby independent gel types or zones are connected as one integrate subject; however, the solvents in the different gels are the same or mutually compatible. For example, as reported by Leibler et al., all the pieces of different hydrogels glued by using various solutions of silica nanoparticles contained water as solvents.<sup>8</sup> In adhesion of host and guest gels reported by Harada and co-workers, water or DMSO was used as solvents for all the gels.<sup>9</sup> Macroscopic hybrid gels have also been prepared by covalent bonding through polymerization of two high viscosity pregel mixtures<sup>11</sup> and “stacking” of one layer of a gel on top of the other through successive atom transfer radical polymerizations (ATRP).<sup>12</sup> In the two cases, identical<sup>11</sup> or mutually compatible solvents<sup>12</sup> were used for the different gels. Incompatible solvents have ever been used in organohydrogel hybrids,<sup>13–16</sup> but they generally

form oil-in-water or water-in-oil emulsions at micro/nanoscale dimensions. Therefore, these organohydrogel hybrids are macroscopically homogeneous. Other hybrid gels have ever been prepared by dispersing one gelator in the other in one solvent, and thereby the products are homogeneous too.<sup>17</sup> To the best of our knowledge, macroscopic hybrids of organogels and hydrogels that are strongly linked at the interface have never been reported.

Herein, we report a unique macroscopic organohydrogel hybrid synthesized by rapid adhesion between the organogel and hydrogel through dynamic covalent chemistry. The hybrid gel obtained was one integrated structure but consisted of two separate macroscopic phases, namely, water and oil. The hydrogel and organogel were prepared by condensation of two poly(ethylene glycol) (PEG) gelators in water and in anisole, respectively, as shown in Figure 1. The acylhydrazone bond, a typical dynamic or reversible covalent bond, acts as cross-linking points in the polymer networks formed in organogels or hydrogels.<sup>18,19</sup> Because of its dynamic chemistry, polymer networks grew across the hydrogel–organogel (water–anisole) interface and connected the two gels in 10 min. Tensile

Received: February 6, 2015

Accepted: April 10, 2015

Published: April 13, 2015

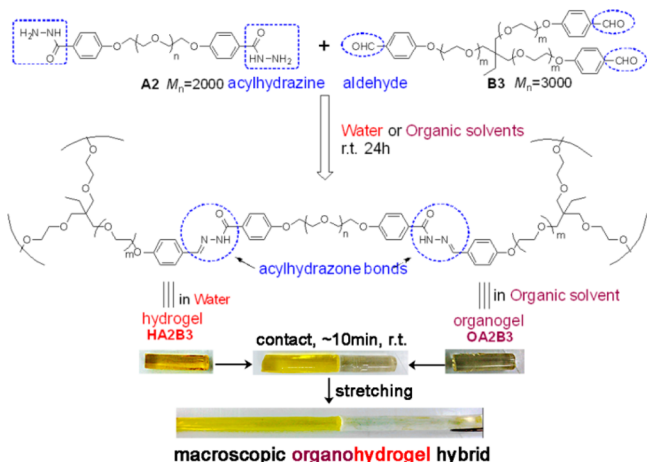


**Figure 1.** Preparation of macroscopic organohydrogel hybrid by rapid adhesion of the hydrogel (HA2B3) and organogel (OA2B3). HA2B3 and OA2B3 contained the same acylhydrazone-bonded polymer networks. HA2B3 was dyed yellow by addition of lemon yellow (0.05 wt %) at the beginning of the preparation. The organic solvent in OA2B3 was anisole.

strength tests proved that the newly formed polymer network at the interface was as strong as that in bulk gels. Therefore, polymer networks in both the hydrogel and organogel are the same in the present study, but they contain immiscible solvents: water in the hydrogel and anisole in the organogel. It was demonstrated that these gels could rapidly self-assemble through dynamic covalent chemistry, and then macroscopic-ordered organohydrogel hybrids could be obtained.

Synthesis of the organogel and hydrogel is shown in Figure 1. The backbones of the gelators A2 and B3 (Figure 1) consist of PEG blocks, which are soluble in water and in anisole. Consequently, the hydrogel and organogel could be prepared directly by mixing the gelators in water and in anisole, respectively. Rheology testing of the gel point showed that the hydrogel HA2B3 formed 35 min after mixing A2 and B3 in water (15 wt % total concentration). However, the organogel OA2B3 could not form in anisole even after 5 h. It formed in 50 min when a minute amount of glacial acetic acid, a catalyst for acylhydrazone condensation, was added in anisole (0.75%, v/v). Therefore, glacial acetic acid (0.75%, v/v) was added in the preparation of all OA2B3 samples. As shown in Figure 1, dynamic acylhydrazone bonds that formed by condensation of the aldehyde and acylhydrazine groups at the chain terminals of A2 and B3 generated the polymer networks.

Mechanical properties of HA2B3 and OA2B3 were studied by a dynamic rheological test after they were aged for 24 h at room temperature. In Figure 2A, the storage modulus ( $G'$ ) and loss modulus ( $G''$ ) of HA2B3 (15 wt %) and OA2B3 (15 wt %) are presented as functions of frequency ( $\omega$ ) at a fixed strain ( $\gamma = 1.0\%$ ). Evidently,  $G'$  for both HA2B3 and OA2B3 reaches a  $\omega$ -independent plateau, and  $G''$  is much lower than  $G'$  in the entire range of  $\omega$  tested (Figure 2A), indicating that HA2B3 and OA2B3 were well-developed gels. However, the curve of  $G''$  for both gels increases after a minimum value with decreasing  $\omega$ , intersecting with that of  $G'$  as expected at lower frequencies, as observed in our previous work.<sup>19,20</sup> This fact implies that acylhydrazone bonds in the polymer networks of HA2B3 and OA2B3 were reversible under the experimental conditions, imparting a self-healing ability to HA2B3 and OA2B3.<sup>18,19</sup>  $G'$  values of HA2B3 (red dots) are much higher

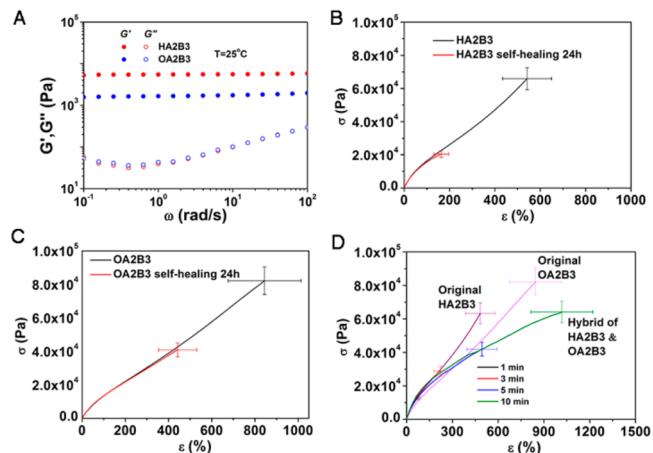


**Figure 2.** (A) Plots of storage modulus ( $G'$ ) and loss modulus ( $G''$ ) versus angular frequency ( $\omega$ ) of HA2B3 and OA2B3 (0.75% HOAc, v/v) at 25 °C. Tensile curves of the gels: (B) Original and self-healed samples of HA2B3. (C) Original and self-healed samples of OA2B3. (D) Organohydrogel hybrid samples of HA2B3 and OA2B3 after adhesion times of 1, 3, 5, and 10 min. The experimental errors for  $\epsilon$  and  $\sigma$  were around  $\pm 20\%$  and  $\pm 10\%$ , respectively. Adhesion was carried out in air at ambient temperature. The concentration of all gels was 15 wt %.

than those of OA2B3 (blue dots). The equilibrium constant ( $K_{eq}$ ) of acylhydrazone formation in different solvents may be calculated from the ratio of the bonding rate constant to the dissociation rate constant ( $k_1/k_d$ ).<sup>20</sup> As shown above, HA2B3 formed in 35 min, whereas OA2B3 needed more time, indicating that  $k_1$  in water might be larger than that in anisole. That is,  $K_{eq}$  in water might be larger than that in anisole although  $k_d$  remains unknown. A higher  $K_{eq}$  value in water implies a higher cross-linking degree in its polymer network and explains the much higher  $G'$  value of HA2B3 compared with that of OA2B3. This result is also consistent with the higher tensile modulus of HA2B3 compared with that of OA2B3 (Figure 2D).

Rapid adhesion between HA2B3 and OA2B3 in atmosphere at room temperature was observed and recorded in a movie (mz5b00096\_si\_002.avi, Supporting Information). As shown in the movie, when a column of HA2B3 (dyed yellow) was attached to a column of OA2B3, a turbid, thin layer at the interface between the hydrogel and organogel columns formed in seconds. This column assembly was then left without external intervention. After about 10 min, the two gel columns merged together. The assembly could not be broken at the turbid interface by pulling at its ends. Instead, it broke at the bulk portion of either HA2B3 or OA2B3 at its failure point. It is noteworthy that adhesion occurred quickly regardless of whether the surfaces of the two gels were fresh or otherwise. In contrast, self-healing of either HA2B3 or OA2B3 required >24 h,<sup>18–20</sup> which is much longer than the time required for adhesion between HA2B3 and OA2B3.

Tensile strength measurements were carried out to quantitatively characterize this rapid adhesion process and to compare it with self-healing of the original gels. As shown in Figure 2B, the break stress of the HA2B3 sample that self-healed for 24 h was  $\sim 20$  kPa, which is  $\sim 30\%$  of its original strength at break, 66 kPa. The break stress of the OA2B3 sample after self-healing for 24 h was 41 kPa, which is 50% of its original strength, 82 kPa (Figure 2C). In contrast, the break

stress of the organohydrogel hybrid sample upon adhesion of HA2B3 and OA2B3 for 10 min reached 64 kPa (Figure 2D), which is almost equivalent to the break strength of the original HA2B3. This result is consistent with the observation that the healed organohydrogel hybrid under stretching often broke at the bulk region of HA2B3 instead of at the interface (mz5b00096\_si\_002.avi, Supporting Information). Stress–strain curves of the organohydrogel hybrid samples after various adhesion times (1, 3, 5, and 10 min) are almost superimposable, but they are different from those of original HA2B3 and OA2B3. It is worth noting that the strain at the break of the organohydrogel hybrid sample (10 min,  $\epsilon$  1000%; Figure 2D) was slightly larger than that of OA2B3 or HA2B3, although the experimental error for this quantity was around 20%.

The structure of the polymer networks of HA2B3 and OA2B3 was observed by IR spectroscopy (Figure S1, Supporting Information). In the spectra of freeze-dried HA2B3 and OA2B3, the  $1690\text{ cm}^{-1}$  peak in the B3 spectrum is absent, indicating that aldehyde end groups in B3 were consumed during condensation with acylhydrazine end groups of A2. C=N stretching vibrations of the formed acylhydrazone bond at  $1620\text{--}1670\text{ cm}^{-1}$  should be present in the spectra of dried HA2B3 and OA2B3, but their peaks overlap with that of C=O in the acylhydrazone bond. A minor shift of the benzene ring peak from  $1600\text{ cm}^{-1}$  (B3) to  $1610\text{ cm}^{-1}$  (dried HA2B3 and OA2B3) reflects the transformation of the CHO group to C=N, which is conjugated with the benzene ring. These observations suggest the formation of the dynamic polymer networks in HA2B3 and OA2B3. The organohydrogel hybrid sample was freeze-dried, and the healed area at the interface was examined by attenuated total internal reflectance Fourier transform infrared (ATR-FTIR) spectroscopy. The ATR-FTIR spectrum at  $1500\text{--}1800\text{ cm}^{-1}$  (green curve in Figure S1, Supporting Information) is not markedly different from that of HA2B3, implying that the polymer network at the interface formed during adhesion was similar to that in the bulk gels.

To prove that the acylhydrazone bond played a key role in the adhesion process, polyurethane organogel and hydrogel in which acylhydrazone is replaced with urethane were prepared. As shown in Figure S2 (Supporting Information), the backbone structures (PEG blocks) of the polyurethane networks in the organogel and hydrogel were similar to those of OA2B3 and HA2B3. The polymer concentration in the gels and the liquid phases (anisole and water) in OA2B3 and HA2B3 were maintained for comparison. The structure of the polymer networks in the polyurethane gels was proved by infrared spectroscopy (Figure S3, Supporting Information). A control experiment showed that adhesion between the polyurethane organogel and hydrogel did not occur even in 48 h (Figure S2 and mz5b00096\_si\_003.avi, Supporting Information). Self-healing of the polyurethane gels was also not observed. These results indicate that adhesion or self-healing was impossible without the acylhydrazone bond.

The turbid, thin layer at the interface between the HA2B3 and OA2B3 columns observed in the movie (mz5b00096\_si\_002.avi, Supporting Information) was highlighted by stereomicroscopic observations (Figure S4, Supporting Information). The appearance of the turbid layer implies that emulsification occurred at the interface of the hydrogel and organogel. HA2B3 labeled with malachite green (MG) dye and OA2B3 were used, and a slice perpendicular to their interface was obtained. Fluorescence microscopy (Figure S5, Supporting

Information) revealed a fluorescent layer at the interface with a thickness of  $\sim 300\text{ }\mu\text{m}$ . Because of the amphiphilicity of MG, it easily accumulated at the oil–water interface. Thus, the fluorescent layer was an emulsion layer. It is worth noting that no emulsion (turbid) layer formed between the polyurethane organogel and hydrogel (Figure S2 and mz5b00096\_si\_003.avi, Supporting Information) and the contacting surfaces upon separation were intact after testing.

The proposed mechanism of rapid adhesion between the hydrogel and organogel is shown in Figure 3. Because the PEG

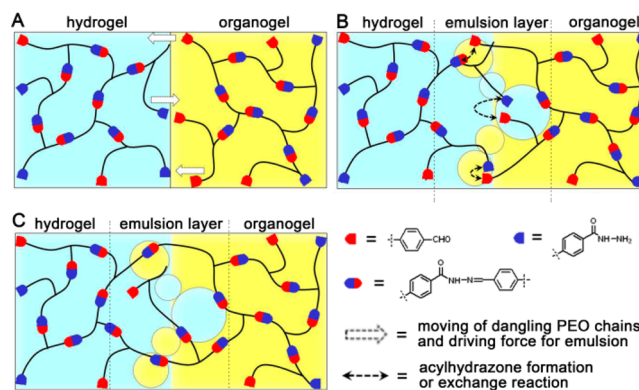


**Figure 3.** Mechanism of rapid adhesion between the hydrogel and organogel. (A) Contact before adhesion. (B) Dangling PEO chains moving across the interface bring solvent to the other phase and form an emulsion layer. (C) Condensation between acylhydrazine and aldehyde end groups, as well as exchange reaction of acylhydrazone, connects the polymer networks in the hydrogel and organogel across the interface.

block is soluble in water and in anisole, it can be a phase transfer agent,<sup>21</sup> and then A2 and B3 chains with acylhydrazine or aldehyde *living* end groups may shuttle back and forth across the hydrogel–organogel interface. As a result, the gelators generate an emulsion layer (turbid layer), which can be an oil-in-water or water-in-oil emulsion, thereby considerably increasing the contact area between the hydrogel and organogel. Meanwhile, acylhydrazone formation and exchange reaction allow growth of dynamic polymer networks across the anisole–water interface. Dangling PEG chains may function as surfactants in the emulsion, stabilizing the interface between the oil and water phases and thereby accelerating the formation of the polymer network. In contrast, no emulsion layer was observed in the control experiment of the polyurethane organogel and hydrogel because there are no acylhydrazine or aldehyde *living* end groups in those gelators. Therefore, we believe that both the emulsion layer and acylhydrazone are critical factors in the adhesion of the two gels that normally repel each other.

Other organic solvents were used to prepare OA2B3, as listed in Table S1 (Supporting Information). The adhesion ability of the organogels thus formed with HA2B3 was examined. The procedure was the same as the anisole case described above. It is found that the rate of adhesion was highly dependent on the organic liquid phase used for OA2B3. Among the organic solvents investigated (Table S1, Supporting Information), only anisole- and chloroform-based organogels resulted in rapid adhesion with HA2B3. One common feature of anisole and chloroform is that they are immiscible with water but can dissolve PEG. However, the other two water-insoluble

solvents, nitroethane and 1,1,2-trichloroethane, did not result in rapid adhesion although PEG is soluble in both; 96 h of adhesion time was needed. It is worth noting that the emulsion layer was observed between HA2B3 and each of the four immiscible solvent-based organogels, but it took much longer time in the case of nitroethane or 1,1,2-trichloroethane. Two water-miscible solvents, dimethylformamide (DMF) and DMSO, were also used as organic phases for OA2B3 in experiments on adhesion with HA2B3. Similarly, a long adhesion time was required: 48 h for DMF gel and 24 h for DMSO gel.

Rapid adhesion between the gels of heterophases is of interest, as this unique feature enabled the selective macroscopic assembly of the gels. OA2B3 and HA2B3 samples with dimensions of 5 mm × 5 mm × 5 mm were prepared, and Rhodamine B was added to the HA2B3 gel pieces to dye them red. When the two kinds of gel pieces (seven pieces for each kind) were mixed in anisole and then shaken for about 5 min, they assembled into the ordered, alternating structure of the organohydrogel (Figure 4A and mz5b00096\_si\_004.avi,

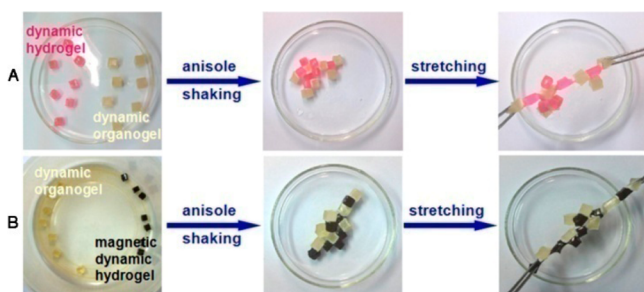


**Figure 4.** Macroscopic self-assembly of organogel and hydrogel. (A) OA2B3 and HA2B3 (dye red by Rhodamine B) shaking in anisole; macroscopic ordered organohydrogel hybrid formed. (B) OA2B3 and magnetic HA2B3 (13 wt %  $\text{Fe}_3\text{O}_4$  nanoparticles) shaking in anisole; macroscopic, ordered, magnetic hydrogel–organogel architecture formed.

Supporting Information). In control experiments, pieces of the pure OA2B3 did not rapidly connect together, and neither did the pure HA2B3. When functional species were loaded in the hydrogel or organogel, various unique macroscopic architectures with fascinating properties could be created through this macroscopic assembly process. For example, after magnetic particles of  $\text{Fe}_3\text{O}_4$  were loaded into HA2B3 and after assembly with OA2B3 was carried out, an architecture with alternating magnetic (black) hydrogel and nonmagnetic organogel domains was produced (Figure 4B and mz5b00096\_si\_005.avi, Supporting Information). As demonstrated by tensile strength tests (also see mz5b00096\_si\_002.avi, Supporting Information), the interface between HA2B3 and OA2B3 was very strong. It is difficult to separate HA2B3 and OA2B3 pieces from the macroscopic gel assembly once it was formed. When the macroscopic gel assembly was pulled from both sides, the HA2B3 gel piece broke without damaging the contact interfaces (mz5b00096\_si\_002.avi, Supporting Information). The results showed again that the adhesion rate of the present system is very high. In the case of self-healing of organogels or hydrogels through dynamic covalent bonding,<sup>18–20,22,23</sup> 2 to 24 h or even longer time is often needed for complete restoration of original mechanical properties, while 10 min is enough to obtain a robust interface with equal mechanical strength of the original gels in the present adhesion

(Figure 2D). The adhesion rate and efficiency are also higher than those of some adhesions through supramolecular interactions, e.g., hydrogen bonding<sup>24</sup> and host–guest interactions in some cases.<sup>25</sup> This fascinating property may facilitate development of hybrid materials with each phase incorporating different functional species.

In summary, we found that hydrogels and organogels, which contain dynamic covalent bonds in their polymer networks, could form macroscopic organohydrogel hybrids by rapid adhesion along the interface of the macroscopic gel pieces. An emulsion layer that rapidly formed at the interface of the organogel and hydrogel increased the contact area between the water and oil phases, accelerating growth of dynamic polymer networks across the interface through acylhydrazone formation and exchange reaction. The fast adhesion and strongly integrated organohydrogel hybrids combined soft materials containing a large volume of water and water-immiscible organic solvent together into a whole object. This adhesion allowed rapid self-assembly of the organogel and hydrogel into ordered architectures. Such a remarkable phenomenon may allow assembly of macroscopic objects having macroscopic phase difference to develop unique smart soft materials.

## ■ ASSOCIATED CONTENT

### 📄 Supporting Information

Experimental details, movies, and additional data. This material is available free of charge via the Internet at <http://pubs.acs.org>.

## ■ AUTHOR INFORMATION

### Corresponding Authors

\*E-mail: ghdeng@scut.edu.cn.

\*E-mail: liucy@iccas.ac.cn.

\*E-mail: chenym35@mail.sysu.edu.cn.

### Notes

The authors declare no competing financial interest.

## ■ ACKNOWLEDGMENTS

This work is financially supported by the NSFC (No. 21174041, 20974034, 21174153) and the Guangdong Natural Science Foundation (No. 10351064101000000).

## ■ REFERENCES

- (1) *Gels handbook*; Osada, Y., Kajiwara, K., Tanaka, T., Ishida, H., Eds.; Elsevier Science & Technology: Amsterdam, 2000.
- (2) Vintilioiu, A.; Leroux, J.-C. *J. Controlled Release* **2008**, *125*, 179–192.
- (3) Drury, J. L.; Mooney, D. J. *Biomaterials* **2003**, *24*, 4337–4351.
- (4) Lee, K. Y.; Mooney, D. J. *Chem. Rev.* **2001**, *101*, 1869–1880.
- (5) Langer, R.; Tirrell, D. A. *Nature* **2004**, *428*, 487–492.
- (6) Burdick, J. A.; Murphy, W. L. *Nat. Commun.* **2012**, *3*, 1269.
- (7) Stuart, M. A. C.; Huck, W. T.; Genzer, J.; Müller, M.; Ober, C.; Stamm, M.; Sukhorukov, G. B.; Szleifer, I.; Tsukruk, V. V.; Urban, M. *Nat. Mater.* **2010**, *9*, 101–113.
- (8) Rose, S.; PrevotEAU, A.; Elzriere, P.; Hourdet, D.; Marcellan, A.; Leibler, L. *Nature* **2014**, *505*, 382–385.
- (9) (a) Harada, A.; Kobayashi, R.; Takashima, Y.; Hashidzume, A.; Yamaguchi, H. *Nat. Chem.* **2011**, *3*, 34–37. (b) Yamaguchi, H.; Kobayashi, Y.; Kobayashi, R.; Takashima, Y.; Hashidzume, A.; Harada, A. *Nat. Commun.* **2012**, *3*, 603. (c) Zheng, Y.; Hashidzume, A.; Takashima, Y.; Yamaguchi, H.; Harada, A. *Nat. Commun.* **2012**, *3*, 831. (d) Zheng, Y.; Hashidzume, A.; Takashima, Y.; Yamaguchi, H.; Harada, A. *ACS Macro Lett.* **2012**, *1*, 1083–1085. (e) Hashidzume, A.; Zheng, Y.; Takashima, Y.; Yamaguchi, H.; Harada, A. *Macromolecules*

- 2013, 46, 1939–1947. (f) Nakamura, T.; Takashima, Y.; Hashidzume, A.; Yamaguchi, H.; Harada, A. *Nat. Commun.* **2014**, 5, 4622.
- (10) Techawanitchai, P.; Ebara, M.; Idota, N.; Asoh, T.-A.; Kikuchi, A.; Aoyagi, T. *Soft Matter* **2012**, 8, 2844–2851.
- (11) Banik, S. J.; Fernandes, N. J.; Thomas, P. C.; Raghavan, S. R. *Macromolecules* **2012**, 45, 5712–5717.
- (12) Yong, X.; Simakova, A.; Averick, S.; Gutierrez, J.; Kuksenok, O.; Balazs, A. C.; Matyjaszewski, K. *Macromolecules* **2015**, 48, 1169–1178.
- (13) Helgeson, M. E.; Moran, S. E.; An, H. Z.; Doyle, P. S. *Nat. Mater.* **2012**, 11, 344–352.
- (14) Kawano, S.; Kobayashi, D.; Taguchi, S.; Kunitake, M.; Nishimi, T. *Macromolecules* **2009**, 43, 473–479.
- (15) Herzig, E. M.; White, K. A.; Schofield, A. B.; Poon, W. C. K.; Clegg, P. S. *Nat. Mater.* **2007**, 6, 966–971.
- (16) Cates, M. E.; Clegg, P. S. *Soft Matter* **2008**, 4, 2132–2138.
- (17) Dasgupta, D.; Srinivasan, S.; Rochas, C.; Ajayaghosh, A.; Guenet, J. M. *Langmuir* **2009**, 25, 8593–8598.
- (18) Deng, G.; Tang, C.; Li, F.; Jiang, H.; Chen, Y. *Macromolecules* **2010**, 43, 1191–1194.
- (19) Deng, G.; Li, F.; Yu, H.; Liu, F.; Liu, C.; Sun, W.; Jiang, H.; Chen, Y. *ACS Macro Lett.* **2012**, 1, 275–279.
- (20) Liu, F.; Li, F.; Deng, G.; Chen, Y.; Zhang, B.; Zhang, J.; Liu, C.-Y. *Macromolecules* **2012**, 45, 1636–1645.
- (21) Zhou, Z.; Alper, H. *Organometallics* **1996**, 15, 3282–3288.
- (22) Wei, Z.; Yang, J. H.; Zhou, J.; Xu, F.; Zrinyi, M.; Dussault, P. H.; Osada, Y.; Chen, Y. M. *Chem. Soc. Rev.* **2014**, 43, 8114–8131.
- (23) (a) Zhang, Y.; Tao, L.; Li, S.; Wei, Y. *Biomacromolecules* **2011**, 12, 2894–2901. (b) Wei, Z.; Yang, J. H.; Du, X. J.; Xu, F.; Zrinyi, M.; Osada, Y.; Li, F.; Chen, Y. M. *Macromol. Rapid Commun.* **2013**, 34, 1464–1470. (c) Amamoto, Y.; Kamada, J.; Otsuka, H.; Takahara, A.; Matyjaszewski, K. *Angew. Chem., Int. Ed.* **2011**, 50, 1660–1663. (d) Imato, K.; Nishihara, M.; Kanehara, T.; Amamoto, Y.; Takahara, A.; Otsuka, H. *Angew. Chem., Int. Ed.* **2012**, 51, 1138–1142.
- (24) Cordier, P.; Tournilhac, F.; Soulie-Ziakovic, C.; Leibler, L. *Nature* **2008**, 451, 977–980.
- (25) Nakahata, M.; Takashima, Y.; Yamaguchi, H.; Harada, A. *Nat. Commun.* **2011**, 2, 511.